

# Observation of Asymmetric Magnetoconductance in Strained 28-nm Si MOSFETs

E. A. Gutiérrez-D., E. Póndigo-de los A., V. H. Vega-G., and F. Guarín

**Abstract**—We have measured gate current components off the axis perpendicular to the surface. The measured gate oxide magnetoconductance exhibits a pronounced magnetic asymmetry, which indicates that the gate current is flowing into different crystallographic orientations with different effective masses and hole mobilities. By identifying and monitoring the different gate current axis components, we have enhanced the understanding of the physics for Si–oxide interface charge transfer and channel conductance in low-dimensional semiconductor devices.

**Index Terms**—Nanoscaled MOSFETs, quantum magnetoconductance.

## I. INTRODUCTION

TO IMPROVE hole mobility on 28-nm p-type Si MOSFET, a rotation of  $45^\circ$ , with respect to the  $\langle 110 \rangle$  crystallographic wafer plane, is implemented in addition to the use of compressive elements [1] that induce strain and provide an extra hole mobility enhancement. Other technologies also make use of retrograde  $\text{Si}_x\text{Ge}_{1-x}$  source and drain extensions to add uniaxial compressive strain [2]. These different technological and structural approaches have led up to 162% improvements for the hole mobility [3]. Even though these device structural changes improve the hole mobility, they give rise to multicrystallographic or anisotropic movement of charges that impact the transport properties along the channel as well as the tunneling of holes through the gate oxide. It is the purpose of this work to introduce an experimental framework that sheds light on the way that holes move through the channel-oxide and oxide-gate interfaces and contribute to the oxide leakage current. For this purpose, an external magnetic field  $B_z$  is applied with different strengths perpendicular to the surface of a 28-nm pMOSFET (see Fig. 1). By doing so, we have observed that, under the reversal of the  $B_z$  field, both the channel and gate currents  $I_s$  and  $I_g$  do not preserve magnetosymmetry [4]. Numerical simulations indicate that this asymmetrical magnetomodulation mechanism is correlated to crystallographic anisotropy and to the morphology of the channel-oxide and gate-oxide interfaces [5].

Manuscript received October 18, 2011; accepted November 18, 2011. Date of publication January 6, 2012; date of current version January 27, 2012. This work was supported in part by CONACyT through Grant 100028. The review of this letter was arranged by Editor M. Östling.

E. A. Gutiérrez-D., E. Póndigo-de los A., and V. H. Vega-G. are with the National Institute of Astrophysics, Optics and Electronics (INAOE), Tonantzintla 72840, Mexico (e-mail: eduardo@inaoep.mx; poae830714@hotmail.com; vic\_hvg@hotmail.com).

F. Guarín is with the Semiconductor Research and Development Center, IBM, Hopewell Junction, NY 12533 USA (e-mail: guarinf@us.ibm.com).

Color versions of one or more of the figures in this letter are available online at <http://ieeexplore.ieee.org>.

Digital Object Identifier 10.1109/LED.2011.2177491

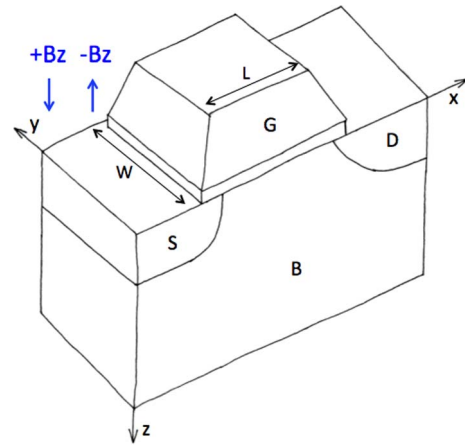


Fig. 1. Experimental setup. The magnetic field ( $B_z$ ) is applied perpendicular to the MOSFET surface in the  $z$ -direction. Channel current  $I_s$  flows in the  $x$ -direction, and gate current  $I_g$  does in the  $z$ -direction.

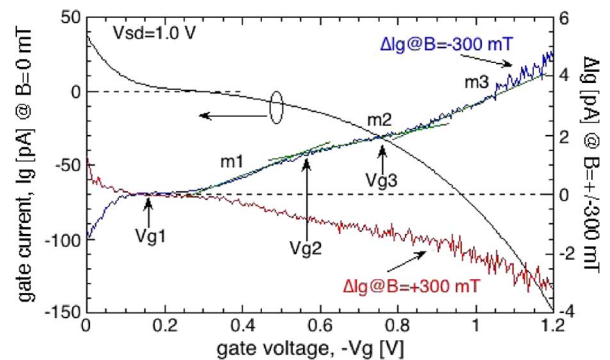


Fig. 2. Measured gate current  $I_g$  and magnetomodulated gate current  $\Delta I_g$  for  $V_{sd} = 1.0$  V and  $B_z = \pm 300$  mT.

## II. EXPERIMENTAL OBSERVATION AND HYPOTHESIS

Static electromagnetic measurements were performed on five samples of a 28-nm pMOSFET with a gate oxide thickness of 1.7 nm and a  $(W/L)$  aspect ratio of  $(1 \mu\text{m}/28 \text{ nm})$ . Following the technique reported in [6], the electrical characteristics were statistically measured, five times in each sample, while the device was assembled in between the poles of an electromagnet that generated a  $B$  field from  $-300$  to  $+300$  mT in steps of 25 mT. Changing the sign of the electromagnet current source changes the  $B$  field direction. The average experimental value of five different samples is used for the analysis. In all the experiments, the magnetic field  $B$  was applied perpendicular to the MOSFET surface.

Fig. 2 shows the measured  $I_g-V_g$  and  $\Delta I_g-V_g$  characteristics at  $V_{sd} = 1.0$  V and  $B = +300$  mT and  $-300$  mT,

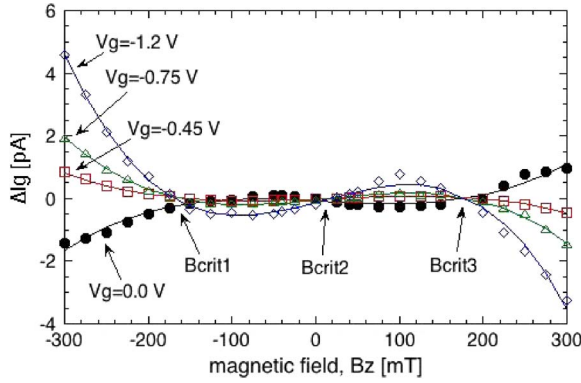


Fig. 3. Measured magnetomodulated gate current  $\Delta I_g$  as a function of the  $B_z$  field for  $V_g = 0.0, -0.45, -0.75,$  and  $-1.2$  V, for  $V_{sd} = 1.0$  V.

where the magnetomodulated gate current is defined as  $\Delta I_g = (I_{gB \neq 0} - I_{gB=0})$ . There are three distinctive  $V_g$  points, i.e.,  $V_{g1}, V_{g2},$  and  $V_{g3}$ , where the slope  $d\Delta I_g/dV_g$  changes. For  $V_g < V_{g1}$ , the  $+B$  field increases the gate leakage current flow from drain to gate, while for  $V_g > V_{g1}$ , the gate-to-channel gate current flows in the reverse direction from gate to channel. Changing the sign of  $B$  reverses the situation, which confirms the magnetoconductance reversibility [4]. The  $V_{g1}$  region correlates to subthreshold channel conduction, while  $V_{g2}$  corresponds with the subthreshold-to-inversion channel conduction transition. The third transition at  $V_{g3}$  is located at the onset of strong inversion. As the  $B_z$  field is parallel to the surface-to-gate axis ( $z$ -axis), the  $(v_{hg} \times B)$  cross product, where  $v_{hg}$  is the gate hole leakage velocity, should be zero. However, the different  $m_1, m_2,$  and  $m_3$  slopes indicate the presence of an  $I_g$  current component off the  $z$ -axis. We have two relevant observations: 1) The off- $z$ -axis  $I_g$  components increase from low to high  $V_g$  voltages, and 2) the magnetodeflection of the  $I_g$   $x$  and  $y$  components is slightly different in magnitude and shape under the reversal of the  $B_z$  field. The second observation reveals that the morphologic structures of the lower channel-oxide and upper gate-oxide interfaces are different, which forces  $I_g$  to have off- $z$ -axis components. By changing the strength of the  $B_z$  field, the magnetodeflection  $\Delta I_g$  should change [4]; the experimental results are shown in Fig. 3, where  $\Delta I_g$  is plotted versus  $B_z$  for different values of  $V_g$ . There is an evident asymmetry for  $V_g = -1.2, -0.75, -0.45,$  and  $0.0$  V. All the curves cross each other and become equal to zero at  $B = -175$  mT,  $B = +0.75$  mT, and  $B = +200$  mT. There is a perfect  $z$ -axis alignment of  $I_g$  and  $B_z$  at these three critical  $B_{crit1}, B_{crit2},$  and  $B_{crit3}$  fields, which indicates a cancellation of the  $x$ - $y$  components. When looking at the magnetomodulated channel current  $\Delta I_s$ , which is expected to be fully perpendicular to  $B_z$ , one should expect a symmetrical reduction of  $I_s$  for negative and positive  $B_z$  fields as dictated by the magnetoconductance mechanism [4]. However, a remarkable anisotropy is also observed, as shown in Fig. 4. Compared to the  $\Delta I_g$  case, the  $\Delta I_s$  magnetomodulated current first increases for positive  $B$  fields in the  $-0.3$  V  $< V_g < -0.7$  V range and then rolls down to negative values for the  $V_g > -0.8$  V range. For negative  $B_z$  fields,  $\Delta I_s$  has a complementary behavior (see Fig. 4). The change of slope from  $m_1$  to  $m_2$  at  $V_{g2}$  in Fig. 2 correlates with the crossing of the extrapolated lines in Fig. 4. This crossing point at  $V_{g2}$

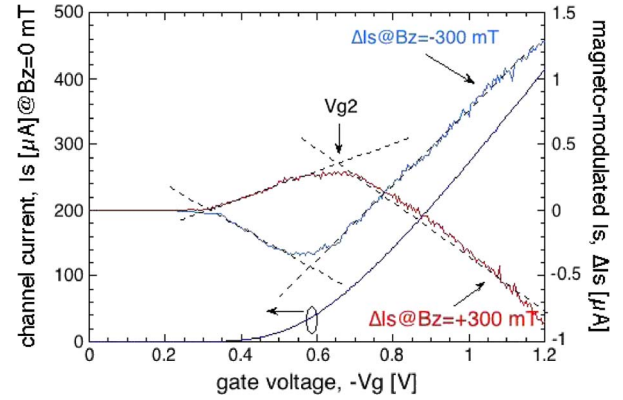


Fig. 4. Measured channel current  $I_s$  and magnetomodulated channel current  $\Delta I_s$  for  $B_z = \pm 300$  mT, for  $V_{sd} = 1.0$  V.

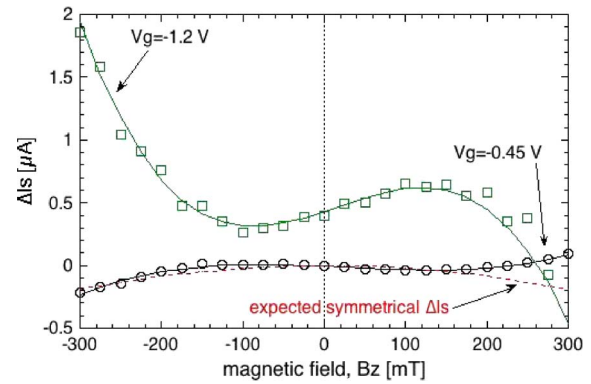


Fig. 5. Measured magnetomodulated channel current  $\Delta I_s$  versus  $B_z$  field for  $V_g = -0.45$  and  $-1.2$  V, for  $V_{sd} = 1.0$  V. The dashed curve represents the expected symmetrical behavior of the  $(\Delta I_s - B_z)$  curve for  $V_g = -0.45$  V.

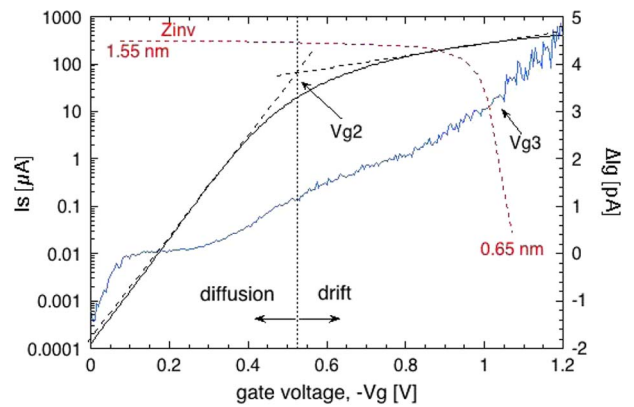


Fig. 6. Measured  $I_s$  and  $\Delta I_g$  as a function of  $V_g$  for  $V_{sd} = 1.0$  V. The inset of the dashed curve represents the simulated inversion hole channel centroid  $Z_{inv}$  varying from  $1.55$  nm at low  $V_g$  to  $0.65$  nm at high  $V_g$ .

corresponds with the diffusion-to-drift transition of the channel conductance (see Fig. 6), which indicates that the magnetic field  $B_z$  has a differentiated effect on the charge diffusion and the drift mechanisms.

The  $\Delta I_g$  magnetomodulated current is larger at high  $V_g$  voltages, which indicates that the  $I_g$  off- $z$ -axis components are larger at high  $V_g$  voltages. The positive values of  $\Delta I_s$  in the  $-0.3$  V  $< V_g < -0.75$  V range for  $+300$  mT and for the  $V_g > -0.75$  V range for  $B_z = -300$  mT indicate a hole flow into different crystal orientations with different mobilities along

the channel. The variation in sign and magnitude of  $\Delta I_s$  as a function of  $V_g$  is explained as a hole channel flow diversion into different crystal orientations. The  $B_z$  field dependence of  $\Delta I_s$  for the diffusion ( $V_g = -0.45$  V) and the drift ( $V_g = -1.1$  V) regions is shown in Fig. 5.

As dictated by the magnetoresistance effect, a parabolic-like behavior (dashed curve) of the  $\Delta I_s - B_z$  curve is expected. However, as observed for both the  $\Delta I_g$  and  $\Delta I_s$ , there is an asymmetrical and nonmonotonic behavior, which is an indication of multidimensional flow of holes both along the channel and through the gate oxide. The data plotted in Fig. 6 confirm the correlation of the inflection  $V_{g2}$  point with the diffusion-to-drift transition. Simulation of the hole inversion channel centroid  $Z_{inv}$  is also plotted as a function of  $V_g$  [7]. This simulation shows  $Z_{inv}$  decreasing with the increase of the absolute value of  $V_g$ , with a strong rolloff at  $V_g = V_{g3}$ . We conclude that the inflection  $V_{g3}$  point and slope  $m_3$  of Fig. 1 are also correlated to the  $Z_{inv}$  position.

### III. CONCLUSION

By using an externally applied magnetic field in conjunction with electrical characterization, we have measured the anisotropic and multicrystallographic nature of hole channel and gate currents in strained 28-nm pMOSFETs. The measured channel and gate magnetomodulated curves  $\Delta I_g - V_g$  and  $\Delta I_s - V_g$  show that the anisotropy and multicrystallographic hole transport is gate voltage dependent. The higher gate voltage leads to higher multicrystallographic hole flow. This is because most of the injected holes into the oxide, at large  $V_g$ 's, come from the source and drain edges, where there is a considerably large  $x-y$   $I_g$  component [5]. On the other hand, the random dopant fluctuation [8] also contributes to the magnetoasymmetry by making the channel charge asymmetrical. We believe that this magnetoconductance characterization technique provides a very powerful tool that contributes to the understanding of the complex charge transport in nanoscaled

semiconductor devices such as single-gate and multigate MOSFETs, Fin-FETs, and quantum wires and dots.

### ACKNOWLEDGMENT

The first author would like to thank IBM for providing the test samples and A. Torres for his insight and very fruitful technical discussions.

### REFERENCES

- [1] F. Arnaud, A. Thean, M. Eller, M. Lipinski, Y. W. Teh, M. Ostermayr, K. Kang, N. S. Kim, K. Ohuchi, J.-P. Han, D.R. Nair, J. Lian, S. Uchimura, S. Kohler, S. Miyaki, P. Ferreira, J.-H. Park, M. Hamaguchi, K. Miyashita, R. Augur, Q. Zhang, K. Strahrenberg, S. ElGhouli, J. Bonnouvrier, F. Matsuoka, R. Lindsay, J. Sudijono, F. S. Johnson, J. H. Ku, M. Sekine, A. Steegen, and R. Sampson, "Competitive and cost effective high-k based 28 nm CMOS technology for low power applications," in *IEDM Tech. Dig.*, 2009, pp. 651–654.
- [2] H. Ohta, Y. Kim, Y. Shimamune, T. Sakuma, A. Hatada, A. Katakami, T. Soeda, K. Kawamura, H. Kokura, H. Morioka, T. Watanabe, J. Oh, Y. Hayami, J. Ogura, M. Tajima, T. Mori, N. Tamura, M. Kojima, and K. Hashimoto, "High performance 30 nm gate bulk CMOS for 45 nm node with  $\Sigma$ -shaped SiGe-SD," in *IEDM Tech. Dig.*, 2005, pp. 240–243.
- [3] M. Yang, E. P. Gusev, M. Ieong, O. Gluschenkov, D. C. Boyd, K. K. Chan, P. M. Kozlowski, C. P. D'Emic, R. M. Sicina, P. C. Jamison, and A. I. Chou, "Performance dependence of CMOS on silicon substrate orientation for ultrathin oxynitride and HfO<sub>2</sub> gate dielectrics," *IEEE Electron Device Lett.*, vol. 24, no. 5, pp. 339–341, May 2003.
- [4] P. Y. Yu and M. Cardona, *Fundamentals of Semiconductors*. New York: Springer-Verlag, 1996, ch. 5, pp. 222–223.
- [5] V. H. Vega-G., "Quantum mechanical analysis and modeling of sub-65 nm MOSFETs under the influence of a magnetic field," Ph.D. dissertation, INAOE, Puebla, Mexico, Oct., 2011.
- [6] E. A. Gutiérrez-D. and F. Guarín, "Experimental evidence of unconventional room-temperature quantum Hall effect (RTQHE) in 65 nm Si nMOSFETs at very low magnetic fields," in *Proc. ESSDERC*, 2010, pp. 178–181.
- [7] J. A. Lopez-Villanueva, P. Cartujo-Cassinello, F. Gamiz, J. Banqueri, and A. J. Palma, "Effects of the inversion-layer centroid on the performance of double-gate MOSFETs," *IEEE Trans. Electron Devices*, vol. 47, no. 1, pp. 141–146, Jan. 2000.
- [8] K. J. Kuhn, M. D. Giles, D. Becher, P. Kolar, A. Kornfeld, R. Kotlyar, S. T. Ma, A. Maheshwari, and S. Mudanai, "Process technology variation," *IEEE Trans. Electron Devices*, vol. 58, no. 8, pp. 2197–2208, Aug. 2011.